16th World Conference on Earthquake, 16WCEE 2017

Santiago Chile, January 9th to 13th 2017

Paper N° 2007

Registration Code: S-F1463214270

CORNER DISPLACEMENT RESPONSE SPECTRA FOR ONE-STOREY ECCENTRIC STRUCTURES

M. Palermo [1], S. Silvestri [2], G. Gasparini [3], T. Trombetti [4]

[1] *Post-doc fellow, Department DICAM, University of Bologna (Italy), michele.palermo7@unibo.it*
[2] *Associate professor, Department DICAM, University of Bologna (Italy), stefano.silvestri@unibo.it*
[3] *Assistant professor, Department DICAM, University of Bologna (Italy), giada.gasparini4@unibo.it*
[4] *Associate professor, Department DICAM, University of Bologna (Italy), tomaso.trombetti@unibo.it*

Abstract

The non-linear response of in-plan asymmetric systems has been extensively studied since the 1980s. Nevertheless, most of the research effort has been devoted to the study of specific asymmetric buildings and, even though relevant progresses have been achieved in the understanding of the complex translational-to-torsional coupled response of such systems, a full knowledge of the seismic behavior of planar asymmetric buildings is still not satisfactory.

To provide results of more general validity, the authors developed a wide parametric study to obtain trends of the response parameters such as maximum displacement and rotations developed by linear and non-linear one-storey asymmetric structures under earthquake ground motion. Based on the results of the parametric study, in the present paper correction factors for the displacement response spectrum are presented.

Keywords: displacement spectra, one-storey asymmetric building, stiff side, flexible side, correction factors

1. Introduction

The behavior of planar asymmetric buildings has been extensively studied since the 1970s. The earliest studies mainly focused on the identification of the controlling parameters considering an elastic structural behaviour (Kan and Chopra [1], Hejal and Chopra [2], Tso [3]). Starting from the 1980s, the attention shifted into the study of the inelastic response of such structures mainly through the development of numerical simulations on selected case studies. Nonetheless, despite the considerable amount of research works, a state-of-the-art dedicated on the behavior of irregular structures (De Stefano and Pintucchi [4]) reported that "*the complexity of inelastic seismic response and the large number of parameters influencing the behavior of irregular buildings, as compared to their elastic counterparts, lead to a lack of general and universally accepted conclusions. Hence, several studies are still aimed at drawing some definitive conclusions.*"

Some results of general validity are represented in the two companion papers by Peruš and Fajfar [5] and Marušić and Fajfar [6] which paved the way for the extended N2 method [7], which represents an extension of the original N2 method (Fajfar and Gašperšič [8]) for in-plan asymmetric buildings which are affected by significant torsional effects. Nevertheless, they recognized that the method could be not so accurate in predicting the displacement demands of torsionally-flexible systems. An alternative nonlinear static approach for asymmetric structures has been developed by Bosco and co-workers [9, 10, 11] by introducing the concept of "corrective eccentricities".

In previous studies, the authors identified a key parameter (referred to as "alpha") depending on two physical properties of the system, namely the eccentricity and the torsional-to-lateral frequency ratio, and related to the attitude of linear-elastic asymmetric systems in developing large rotational responses. Based on the "alpha" parameter, a simplified method (the so-called "alpha" method) has been proposed for the prediction of the maximum torsional response of one-storey linear asymmetric structures under seismic excitation (Trombetti and Conte [12] and Palermo et al. [13]). More recently, the authors conducted a large parametric study aimed at identifying the main trends of the seismic response of both elastic and inelastic one-storey asymmetric structures accounting for the influence of different damping ratios and ductility demands (Palermo et al. [14]). In the present study, the results of the parametric study are used to introduce correction factors for corner-side displacement spectra of asymmetric buildings.

2. The parametric study

2.1 The one-storey linear asymmetric system and its non-linear counterpart

Let us briefly describe the one-storey linear eccentric structure (i.e. a system characterized by non-coincident centre of mass, CM, and centre of stiffness, CK, leading to a one-way eccentricity E_x=E, E_y=0) and its non-linear counterpart which were extensively studied in the past by the authors (Fig. 1a and b).

With reference to the linear system of Fig.1a, it is assumed that the diaphragm is infinitely rigid in its own plane, and that the lateral-resisting elements are massless and axially inextensible. The self torsional stiffness (k_θ) of each lateral-resisting element is neglected. Under these assumptions, the linear system can be modelled as a 3-dof system: the longitudinal centre of mass displacement, $u_{y,CM}$; the transversal centre of mass displacement, $u_{x,CM}$; the centre of mass rotation, $u_{\theta,CM}$ (coincident with the floor rotation, u_θ).

The non-linear system of Fig. 1b is the same one which was first extensively studied by Goel and Chopra [15] and consists of a roof diaphragm, assumed to be rigid in its own plane, supported by three frames, namely A, B and C (Fig.1 b). Frame A is oriented along the y-direction, at a distance E from the centre of mass (CM). Frames B and C are oriented along the x-direction, located at the same distance D/2 from the CM. Frames B and C are assumed to have the same lateral stiffness (k/2) so that the system is not eccentric along the y-direction. Frame A is assumed to have a lateral stiffness equal to k. Each frame is characterized by an elastic-perfectly plastic response. The yield strength F_y is obtained by imposing a force reduction factor R (see Fig. 1b). Along the x-direction the eccentricity is equal to E. The rigid motion of the roof can be described by the three degrees of freedom defined at the CM of the slab: displacements u_x (in the x-direction) and u_y (in the y-direction), and torsional rotation u_θ (about the vertical axis).

The dynamic behaviour of the two systems is mainly governed by the following key parameters:

- the normalized eccentricity $e=E/L$,
- the torsional-to-lateral frequency ratio Ω_θ,
- the uncoupled longitudinal period T_L from 0.1 s to 3.0 s,
- the damping ratio ξ ,
- the force reduction factor R.

The seismic behavior of the two systems has been analyzed by performing a wide parametric study, by varying the system parameters as summarized in Table 1.

Table 1 – Ranges of the key parameters

parameter	e	Ω_θ	T_L [s]	ξ	R
ranges	0.00 - 0.50	0.1 - 2.0	0.1 - 3.0	2% - 30%	2 - 5

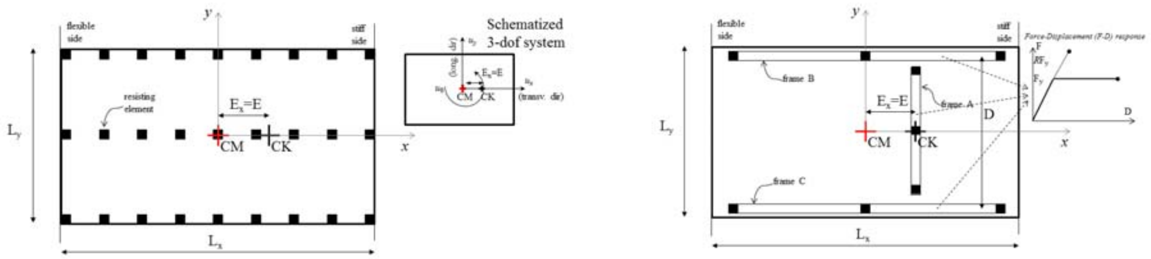

(a) (b)

Fig. 1 – Linear (a) and non-linear (b) one-storey asymmetric system.

2.1 The seismic input and the response parameters

An ensemble of 50 ground motions selected from the PEER database has been used to perform the seismic analyses. The ground motions have been selected with shear wave velocity Vs,30 in the range of 360m/s to 800m/s (i.e. soil type B according to EC8). The seismic input is applied along the longitudinal direction (namely, the y-direction). A total number of 728000 linear time-history analyses and 416000 non-linear time history analyses have been performed using an ad-hoc MATLAB code. The results of the parametric study were described in terms of various normalized (with respect to the maximum center mass displacement) response parameters measuring (i) the amplitude of the rotational responses, (ii) the correlation between displacement and rotational responses, (iii) the increase in the overall displacement demand due to the so-called period shifting effect (Palermo et al. 2013 [13]), (iv) the maximum corner side displacements. Among all the considered response quantities, the magnification (or correction) factors, $M_{CM,s}$ and $M_{CM,f}$, of the maximum corner side displacements with respect to the centre of mass displacement are here further analyzed:

$$M_{CM,s} = \frac{u_{y,s,\max}}{u_{y,CM,\max}} \tag{1}$$

$$M_{CM,f} = \frac{u_{y,f,\max}}{u_{y,CM,\max}} \tag{2}$$

where $u_{y,s,\max}$ and $u_{y,f,\max}$ are the maximum corner displacements developed during the earthquake excitation at the so-called stiff side (e.g. the closer to CK) and at the flexible side, (e.g. the farther from CK). $u_{y,CM,\max}$ represents the maximum longitudinal centre of mass displacement developed during the earthquake excitation.

3. 3D surfaces of $M_{CM,s}$ and $M_{CM,f}$ response parameters

The trends of the response parameters $M_{CM,s}$ and $M_{CM,f}$ with respect to e and Ω_θ are represented through 3D surfaces with fixed value of T_L. A complete description of such 3D surfaces is provided in the work by Palermo et al. [14]. For instance, Figures 2 and 3 show the surfaces of $M_{CM,s}$ and $M_{CM,f}$ for a short period (T_L=0.3 s) and a long period (T_L=2 s) linear structure and four different damping ratios. Similar surfaces are shown in Figures 4 and 5 for the corresponding short period (T_L =0.3 s) and long period (T_L =2 s) nonlinear structure characterized by four different force reduction factors.

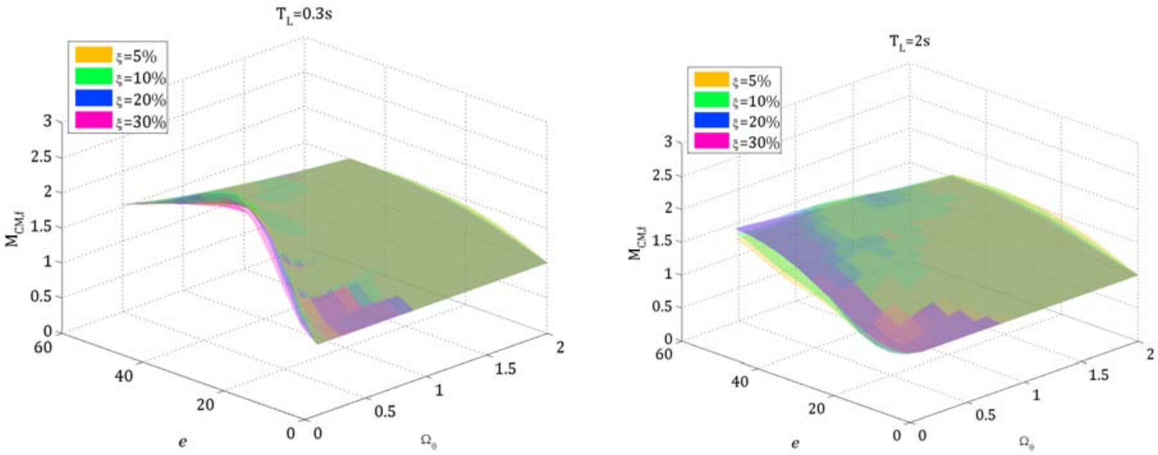

(a) (b)

Fig. 2 – Surfaces of $M_{CM,f}$ for linear systems with (a) T_L=0.3 s and (b) T_L=2 s.

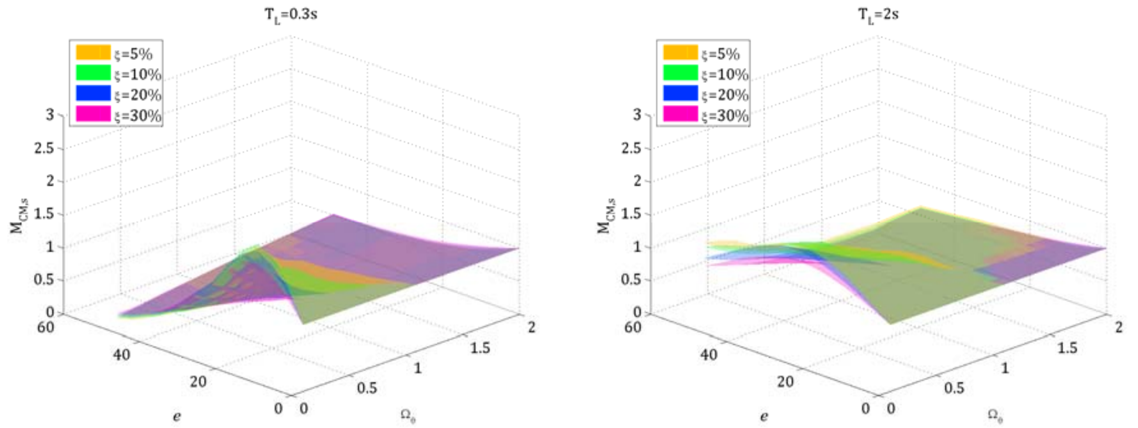

(a) (b)

Fig. 3 – Surfaces of $M_{CM,s}$ for linear systems with (a) T_L=0.3 s and (b) T_L=2 s.

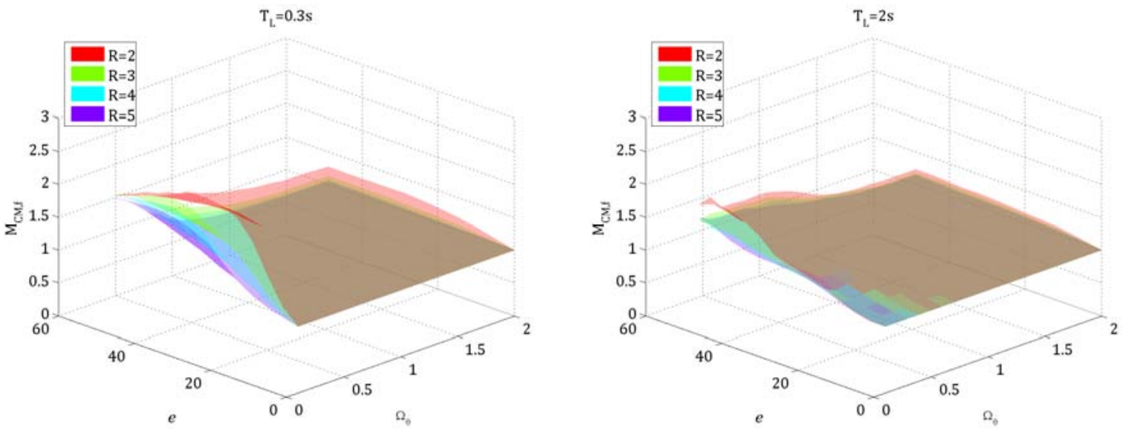

(a) (b)

Fig. 4 – Surfaces of $M_{CM,f}$ for nonlinear systems with (a) T_L=0.3 s and (b) T_L=2 s.

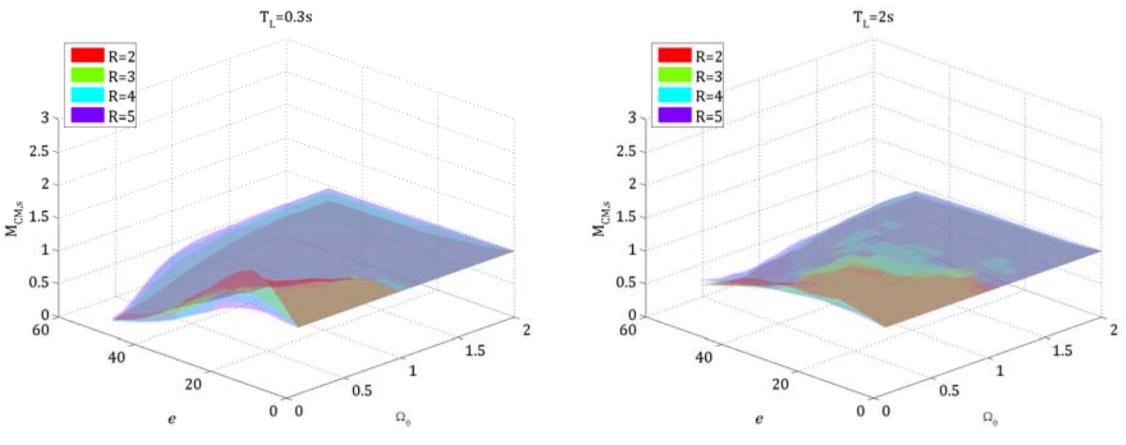

(a) (b)

Fig. 5 – Surfaces of $M_{CM,s}$ for nonlinear systems with (a) T_L=0.3 s and (b) T_L=2 s.

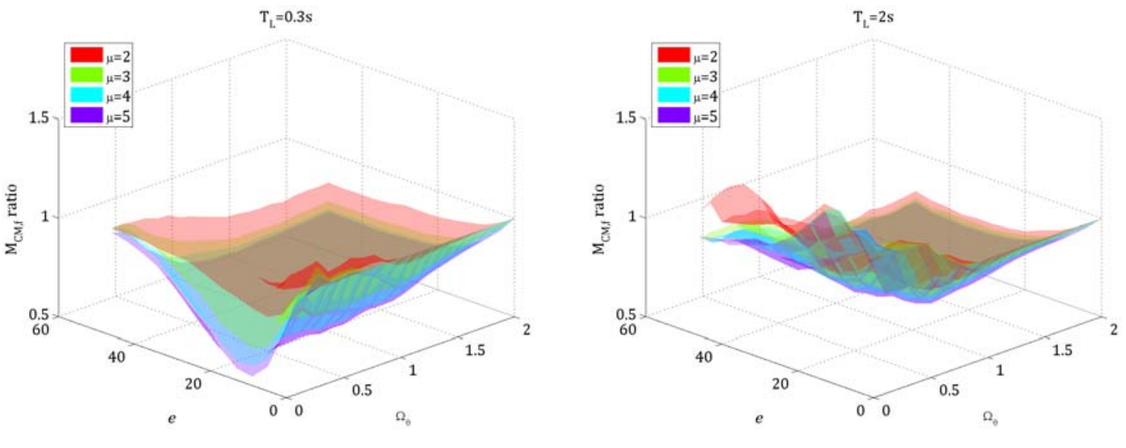

(a) (b)

Fig. 6 – Surfaces of $M_{CM,f}$ ratio: nonlinear systems / linear response. (a) T_L=0.3 s and (b) T_L=2 s.

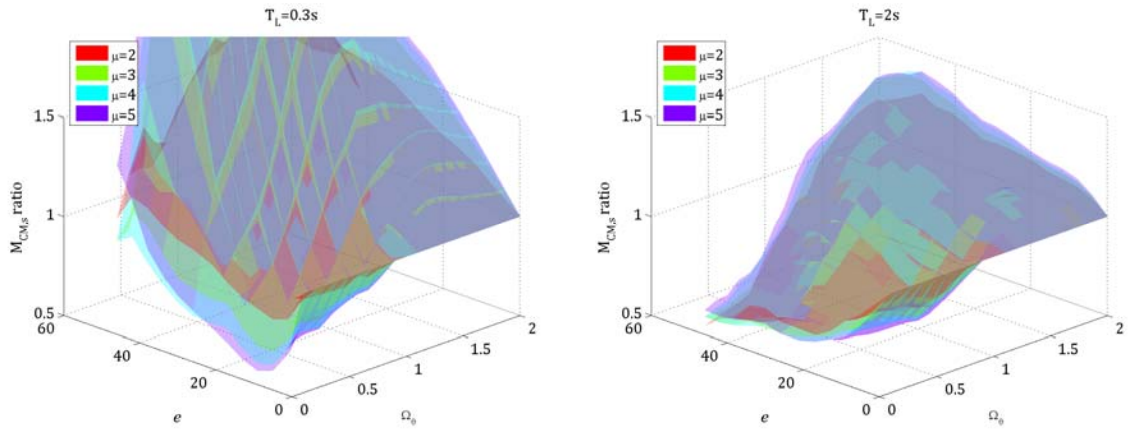

(a) (b)

Fig. 7 – Surfaces of $M_{CM,s}$ ratio: nonlinear systems / linear response. (a) T_L=0.3 s and (b) T_L=2 s.

First, it can be noted that linear and non-linear systems have qualitatively similar trends of $M_{CM,s}$ and $M_{CM,f}$.

The ratios between the non-linear (for a 5% damping ratio) and the linear structural responses of parameters $M_{CM,s}$ and $M_{CM,f}$ are shown in Figures 6 and 7, respectively, and allow to better appreciate the influence of the force reduction factor. In more detail:

- Maximum amplifications around 2.0-2.5 are observed at the flexible side for systems characterized by short T_L, low Ω_θ and moderate e.
- Maximum amplifications around 1.5-2.0 are observed at the stiff side for systems characterized by short T_L, low Ω_θ and small e.
- In the linear case, the damping ratio seems to have a small influence on the linear response surfaces.
- The non-linear surfaces appear smother and have reduced peaks with respect to the linear ones. For increasing values of force reduction factor, the peaks tend to decrease.
- The displacement magnifications at the flexible side are reduced in case of non-linear behaviour. On the contrary, especially for short period structures, the maximum non-linear displacements at the stiff side may increase with respect to the corresponding maximum linear displacements.

4. Correction factors for inelastic corner-side displacement spectra

The results of the wide parametric study briefly summarized in the previous section constitutes a body of knowledge which can be used to introduce new tools for an in-depth comprehension and also a quantitative evaluation of specific response quantities. For instance, the response parameters $M_{CM,s}$ and $M_{CM,f}$ could be represented through 3D spectra, i.e. as function of the uncoupled natural period T_L and eccentricity e (for fixed values of Ω_θ). Then, from the 3D spectra, standard (i.e. 2D) response spectra of $M_{CM,s}$ and $M_{CM,f}$ can be obtained. This spectra representation is much more useful for professional designer, since the response spectrum of $M_{CM,s}$ and $M_{CM,f}$ can be easily coupled to the standard response spectrum in order to evaluate earthquake displacement demands at the corner sides. Examples of elastic and inelastic 3D spectra of $M_{CM,s}$ and $M_{CM,f}$ are given in Fig. 8. In general, the surfaces of the inelastic spectra appear smother, particularly for torsionally stiff systems, with respect to the linear elastic counterparts. Also the peaks have reduced values. In the next section, attention will be focused in the inelastic spectra with the purpose of providing simplified analytical expressions.

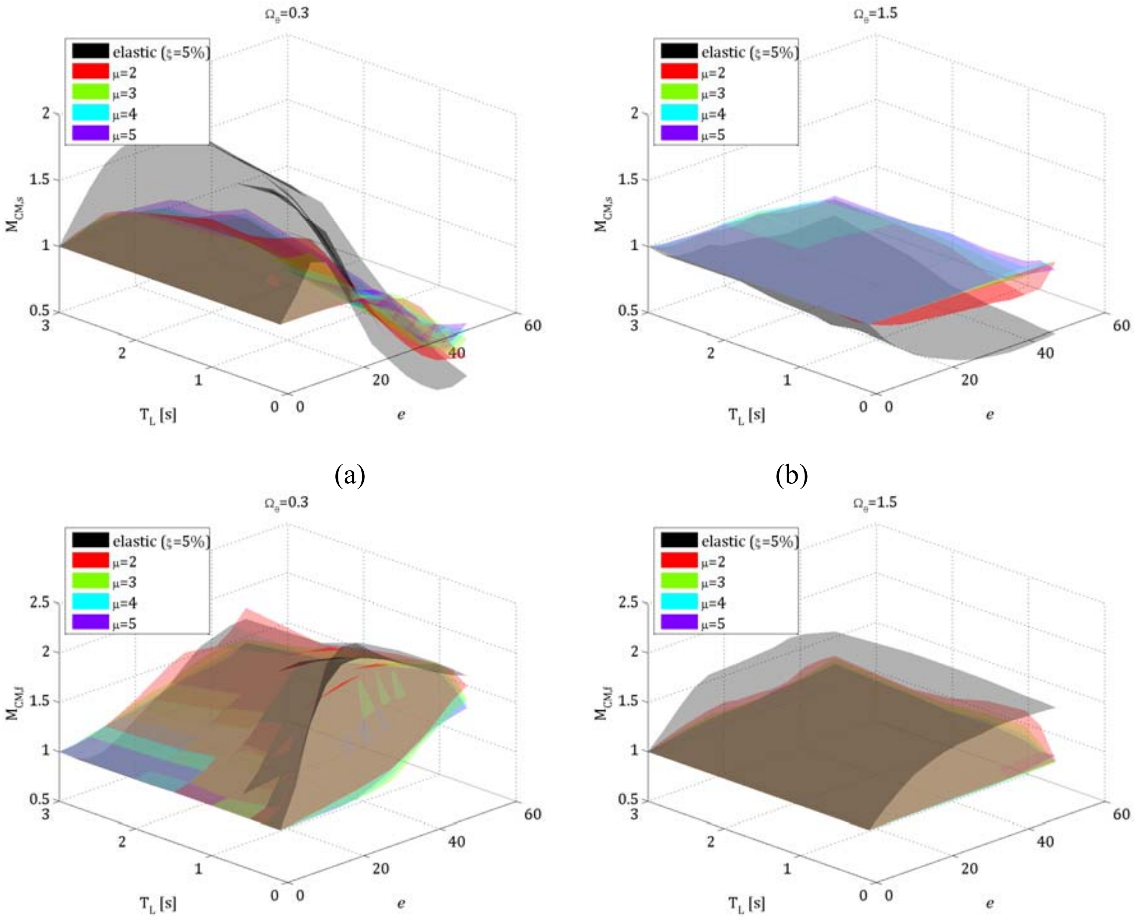

(a) (b) (c) (d)

Fig. 8 – 3D spectra of: (a) $M_{CM,\mathrm{s}}$ for torsionally flexible system with Ω_θ =0.3; (a) $M_{CM,\mathrm{s}}$ for torsionally stiff system with Ω_θ =1.5; (a) $M_{CM,f}$ for torsionally flexible system with Ω_θ =0.3; (a) $M_{CM,f}$ for torsionally stiff system with Ω_θ =1.5.

4.1 $M_{CM,s}$ and $M_{CM,f}$ inelastic response spectra

The $M_{CM,s}$ and $M_{CM,f}$ values as obtained from the nonlinear analyses are represented as response spectra, i.e. as function of uncoupled natural period T_L (and fixed values of e, Ω_θ and R). Examples of $M_{CM,f}$ inelastic response spectra are shown in Fig. 9.

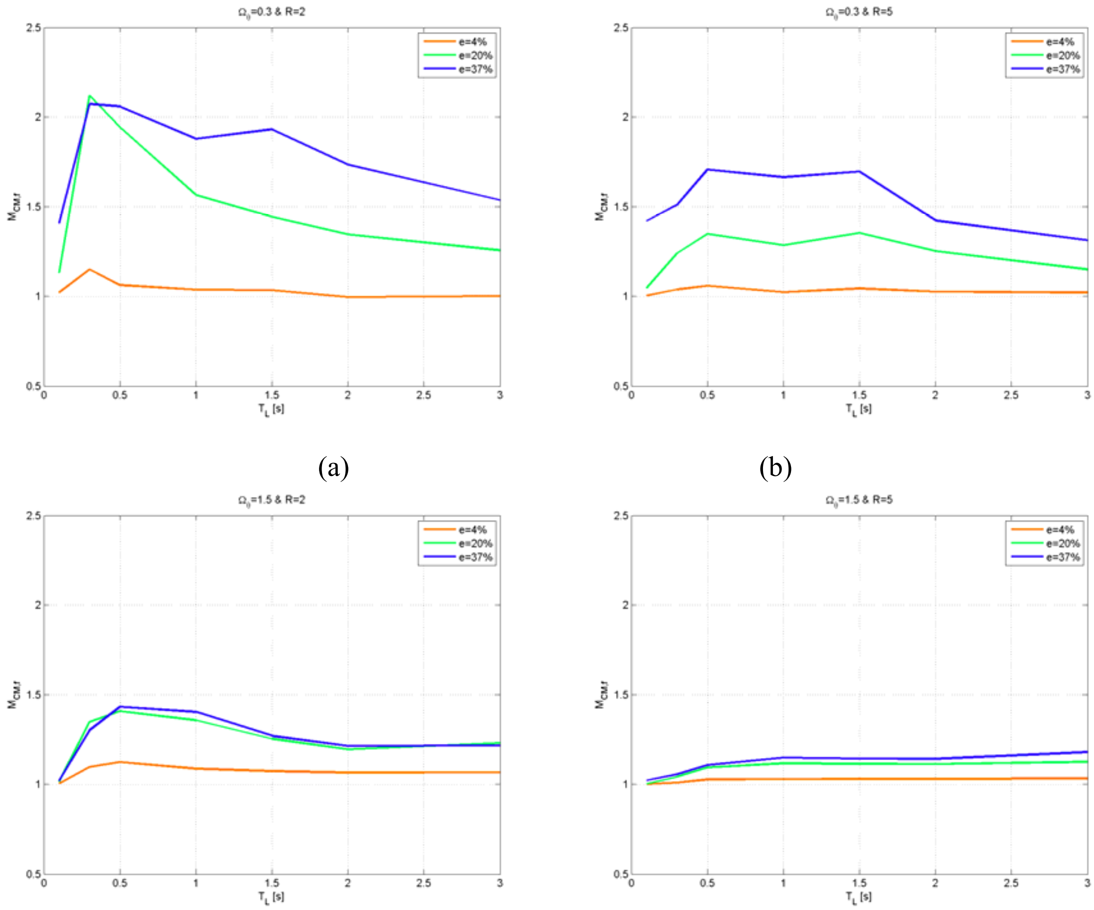

(a) (b) (c) (d)

Fig. 9 – $M_{CM,f}$ spectra for: (a) Ω_θ =0.3, R=2; (b) Ω_θ =0.3, R=5; (c) Ω_θ =1.5, R=2; (d) Ω_θ =1.5 and R=5.

4.2 An analytical formulation for $M_{CM,s}$ and $M_{CM,f}$ spectra

The following functional form of $M_{CM,s}$ and $M_{CM,f}$ spectra is here proposed:

$$\mathrm{M}(T_L) = b_1 + b_2 \cdot T_L + \frac{b_3}{T_L} \tag{3}$$

In Fig. 10, selected spectra of $M_{CM,s}$ and $M_{CM,f}$ according to Eq. (3) are compared to those obtained from numerical simulations. It can be noted that Eq. (3) is adequate to approximate the spectra of $M_{CM,s}$ and $M_{CM,f}$.

Coefficients b_1, b_2, b_3 depend on e, Ω_θ, and R and are calibrated through nonlinear regression analyses (Fig. 11). However, from a design perspective they could be expressed by families of step-wise linear functions of e:

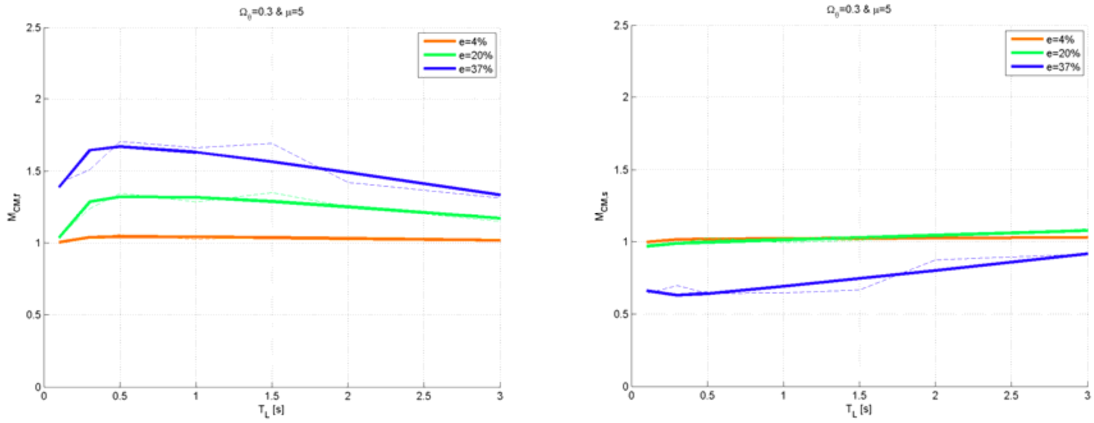

(a) (b)

Fig. 10 – (a) $M_{CM,f}$ and (b) $M_{CM,s}$ according to Eq. (3) compared with the corresponding numerical spectra.

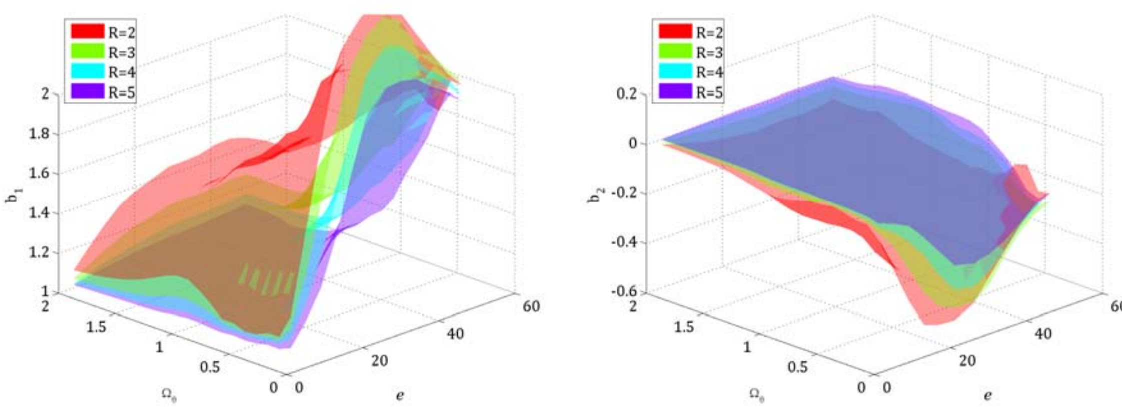

(a) (b)

Fig. 11 – Coefficients (a) b_1 and (b) b_2 vs e and Ω_θ.

$$b_j(e,\mu) = \alpha + \beta \cdot \frac{e}{\mu^\gamma} \tag{4}$$

with j=1, 2, 3; α=1 for j=1 and α=0 for j=2, 3. β and γ values are different for the following classes of buildings: torsionally-stiff, torsionally-flexible, and for small or large eccentricities (for a total of 4 classes). The explicit equations of b_1, b_2 and b_3 for the different classes of buildings will be presented in a future work.

5. An applicative example

The structures analyzed by Marušić and Fajfar 2005 are here considered to evaluate the effectiveness of using $M_{CM,s}$ and $M_{CM,f}$ correction factors to estimate displacement demands at corner side of planar asymmetric buildings. S-15 and F2-15 are the considered structures. The symmetric structures S and F1 (not considered in the study) were designed according to pre-standards Eurocode 3 and 8 [16, 17] by Mazzolani and Piluso [18]. They are both torsionally-stiff buildings with the first two modes predominantly translational and the third mode predominantly torsional. In structure S all the beam-to-column connections are moment-resistant, while in structure F1 moment-resistant connections are only in the frames at the corner bays at the perimeter. The structure F2 consists of the same moment-resisting frames as those of structure F1, but they are located in the interior of the plan, thus resulting in a torsionally-flexible system. A 15% eccentricity between the center of the stiffness (coincident with the geometrical center of the square plane of the buildings) and the center of the mass along the x-direction is considered here by applying different gravity loads in the different portion of the floors. Beams and columns are made by structural steel. The first three natural periods of the eccentric buildings S-15 and F2-15 and corresponding not eccentric ones (namely S-0 and F2-0) are collected in Table 2.

3D finite element models of the buildings are developed using the commercial software SAP 2000 v16.1.1. Plastic hinges are placed at the ends of all columns and beams so that system may experience inelastic responses. The seismic weight W_{tot} of the two structures is around 16000 kN. The base shear V_{base} at the first yielding is around 4000 kN for both structures, thus leading to a V_{base} / W_{tot} ratio of around 0.25. The structures are subjected to the El-Centro 1940 North-South Component record, which is applied along the *y*-direction. In order to evaluate the structural response within both the elastic and the inelastic fields, the amplitudes of the ground motions are scaled by applying a scaling factor ranging from 2 to 6 to the unscaled record (peak ground acceleration of 0.3). Based on the dynamic properties and strengths of the buildings it is expected that both buildings would respond essentially within the elastic field when subjected to the unscaled El-Centro record, while they would experience inelastic responses when subjected to the scaled ground motions.

The maximum displacement responses at the roof level as obtained from the different time history analyses (e.g. unscaled El Centro, and scaled El Centro with scaling factors equal to 3, 4, 6) as normalized with respect to the corresponding maximum centre of mass displacement are shown in Fig. 13 with solid lines. Also $M_{CM,f}$ and $M_{CM,s}$ factors as given by Eq. (3) are shown in the same graphs for four different R values. It can be noted that the analytical expressions of $M_{CM,f}$ and $M_{CM,s}$ are able to capture the trends of the numerical responses. Of course, in order to verify the effectiveness of the $M_{CM,f}$ and $M_{CM,s}$ spectra here introduced a large number of verification examples have to be developed. Such a verification study will be the objective of a future work.

Table 2 – Natural periods of buildings S-0, S-15, F2-0 and F2-15.

Period	S-0	S-15	F2-0	F2-15
T_1 [s]	1.40	1.53	1.75	1.87
T_2 [s]	1.40	1.40	1.38	1.38
T_3 [s]	1.18	1.02	1.38	1.22

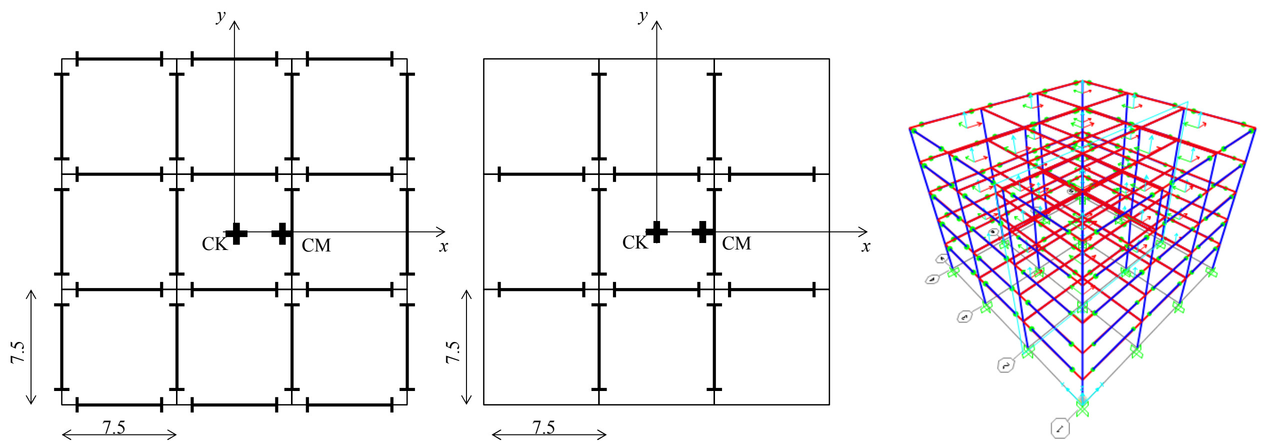

(a) (b) (c)

Fig. 12 – Schematic plans of (a) S-15 and (b) F2-15. (c) SAP 2000 model of F2-15.

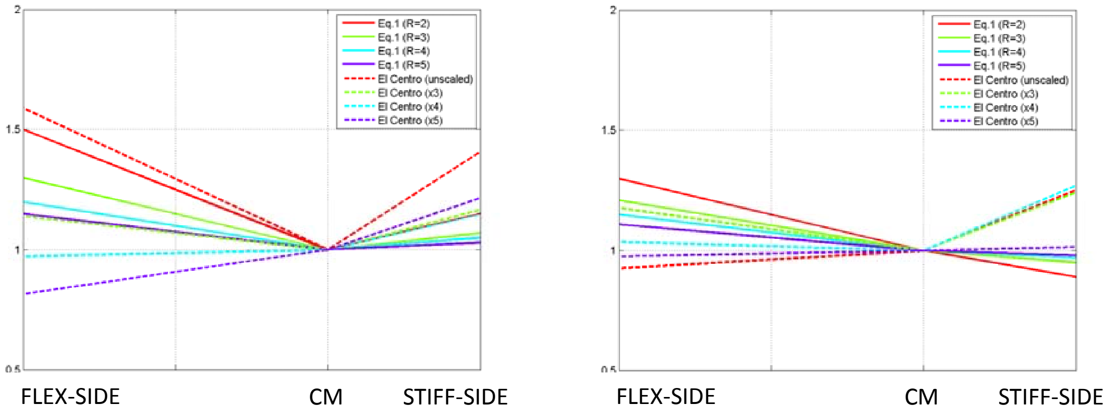

(a) (b)

Fig. 13 – Normalized displacements $u_{max}/u_{CM,max}$ in the horizontal plane at the top of buildings and predictions according to Eq. (1): (a) F-15 building; (b) S-15 building.

6. Conclusions

In the present paper, response spectra of the normalized corner-side displacement response (e.g. maximum stiff side and flexible side displacements divided by the maximum center mass displacement) are introduced as correction factors which can be coupled to the displacement spectra to more precisely estimate the earthquake displacement demands of planar asymmetric buildings. Such correction factors are derived from the results of a previous wide parametric study aimed at assessing the seismic behavior of elastic and inelastic one-storey asymmetric buildings by varying their key parameters in order to cover most of the realistic cases. Furthermore, an analytical formulation of such correction factors is proposed. It is found that the proposed simple analytical form is suitable to reasonably approximate the numerical results. Nonetheless, a further calibration of the coefficients has to be carried out to obtain fully analytical expressions to be used for design purposes. The analytical formulations of the spectra of the correction factors could be easily incorporated in future building codes for a better estimation of the seismic displacement demands of planar asymmetric buildings.

7. References

[1] Kan CL, Chopra AK (1987): Linear and non linear earthquake responses of simply torsionally coupled systems, Earthquake Engineering Research centre, University of California, Berkeley, CA.

[2] Hejal R, Chopra AK (1987): Earthquake response of torsionally coupled buildings. Report UCB/EERC 87/20, Earthquake Engineering Research Center, University of California, Berkeley, CA.

[3] Tso WK (1990): Static eccentricity concept for torsional moment estimations. *Journal of Structural Engineering ASCE,* **116**(5), 1199–121.

[4] De Stefano M, Pintucchi B (2008): A review of research on seismic behaviour of irregular building structures since 2002. *Bulletin of Earthquake Engineering*, **6**(2), 285-308.

[5] Perus I, Fajfar P (2005): On the inelastic torsional response of single-storey structures under bi-axial excitation. *Earthquake Engineering and Structural Dynamics*, **34**, 931–941.

[6] Marušić D, Fajfar P (2005): On the inelastic seismic response of asymmetric buildings under biaxial excitation. *Earthquake Engineering and Structural Dynamics*, **34**, 943-963.

[7] Fajfar P, Kilar V, Marusic D, Perus I, Magliulo G (2002): The extension of the N2 method to asymmetric buildings. Proceedings of the Fourth Forum on Implications of Recent Earthquakes on Seismic Risk, Technical Report TIT/EERG, 02/1. Tokyo Institute of Technology: Tokyo, 291–308.

[8] Fajfar P, Gašperšič P (1996): The N2 method for the seismic damage analysis of RC buildings. *Earthquake Engineering and Structural Dynamics*, **25**(1), 31-46.

[9] Bosco M, Ferrara G, Ghersi A, Marino EM (2009): Corrective eccentricities for the evaluation of the seismic response of one-storey asymmetric systems by nonlinear static analysis. *Environmental Semeiotics*; **2**, 80–94.

[10] Bosco M, Ghersi A, Marino EM (2012): Corrective eccentricities for assessment by the nonlinear static method of 3D structures subjected to bidirectional ground motions. *Earthquake Engineering and Structural Dynamics*, **41**(13), 1751-1773.

[11] Bosco M, Marino EM, Rossi PP (2013): An analytical method for the evaluation of the in-plan irregularity of non-regularly asymmetric buildings, *Bulletin of Earthquake Engineering,* doi:10.1007/s10518- 013-9438-3

[12] Trombetti T, Conte JP (2005): New insight into and simplified approach to seismic analysis of torsionally coupled one-storey, elastic systems, *Journal of Sound and Vibration* **286**, 265-312.

[13] Palermo M, Silvestri S, Gasparini G, Trombetti T (2013): Physically-based prediction of the maximum corner displacement magnification of one-storey eccentric systems. *Bulletin of Earthquake Engineering*, **11**(5), 1467-1491.

[14] Palermo M, Silvestri S, Gasparini G, Trombetti T (2016): Maximum Corner Displacement Amplifications for Inelastic One-Storey In-Plan Asymmetric Systems Under Seismic Excitation. In Seismic Behaviour and Design of Irregular and Complex Civil Structures II (pp. 243-254). Springer International Publishing.

[15] Goel RK, Chopra AK (1990): Inelastic seismic response of one storey, asymmetric plan systems: Effects of stiffness and strength distribution, *Earthquake Engineering and Structural Dynamics*, **19**(7), 949-970.

[16] Eurocode 3. Design of steel structures. European Prestandard ENV 1993. CEN: Brussels, 1992.

[17] Eurocode 8. Design provisions for earthquake resistance of structures. European Prestandard ENV 1998. CEN: Brussels, 1994.

[18] Mazzolani FM, Piluso V (1997): The influence of the design configuration on the seismic response of moment-resisting frames. Behaviour of Steel Structures in Seismic Areas: STESSA'97, Kyoto, Mazzolani FM, Akiyama H (eds); Edizioni: Salerno.